

DOA ESTIMATION OF MULTIPATH WAVES USING 2D-ESPRIT WITH TRIANGULAR ANTENNA ARRAY

Toru KURODA Nobuyoshi KIKUMA Naoki INAGAKI
 Department of Electrical and Computer Engineering
 Nagoya Institute of Technology
 Gokiso-cho, Showa-ku, Nagoya 466-8555, Japan
 E-mail: kuroda@maxwell.elcom.nitech.ac.jp

1 Introduction

Recently we can see the rapid development of wireless communications, and so there are great demands for measurement and analysis of radio propagation structure to realize the highly reliable and flexible communication systems. To understand the propagation structure, it is much effective to know the signal parameters (DOA, TOA, strength, and so on) of the individual incoming waves at receiving points.

For the purpose, many signal processing algorithms have been investigated, and MUSIC and ESPRIT are employed very often because they have high resolution in separating the received waves[1][2][3]. Among them, the superresolution estimator such as Unitary ESPRIT attracts much attention because of its high computational efficiency, and furthermore it is significantly extended to the multi-dimensional algorithm so as to obtain the multiple signal parameters at the same time[4]. However, this type of estimator imposes great restrictions on the array configuration. For example, it must be an equispaced linear array or rectangular array[4].

Therefore, this paper proposes the 2D-ESPRIT estimator applicable to triangular antenna arrays which are popularly used but cannot be utilized by Unitary ESPRIT. In addition, via computer simulation, we discuss the performance of the proposed algorithm in 2D-DOA(azimuth and elevation angles) estimation.

2 Estimation Principle

2.1 Receiving system and signal models

Figure 1 shows the triangular antenna array with $M (= M_1(M_1 + 1)/2)$ identical elements placed in the $x-y$ plane, where $M_1 = M_2$ in this paper. The element spacing is Δu and Δy in the u -axis and y -axis, respectively. For simplicity, it is assumed that all elements have identical characteristics. We consider here the estimation of 2D-DOAs(θ and ϕ) of L narrowband plane waves impinging on the array, which are defined in Fig.2.

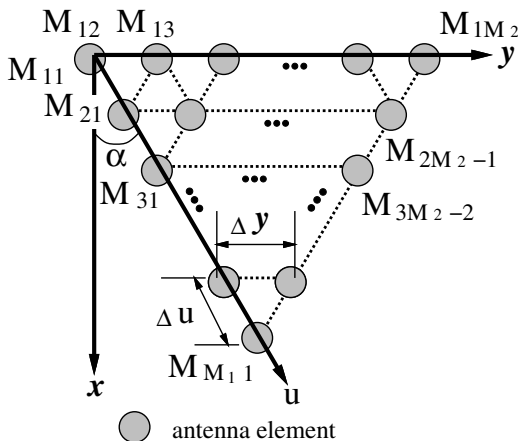


Figure 1: Triangular Antenna Array

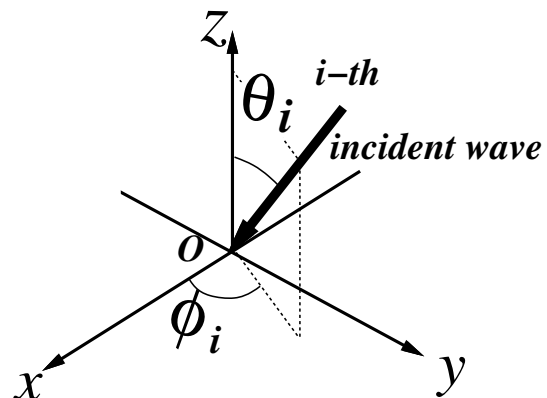


Figure 2: 2D-DOA of incident wave

2.2 Principle of 2D-ESPRIT

Since 2D-ESPRIT requires two identical subarrays, we extract subarray 11 and subarray 12 along the u -axis and subarray 21 and subarray 22 along the y -axis, which are depicted in Fig.3.

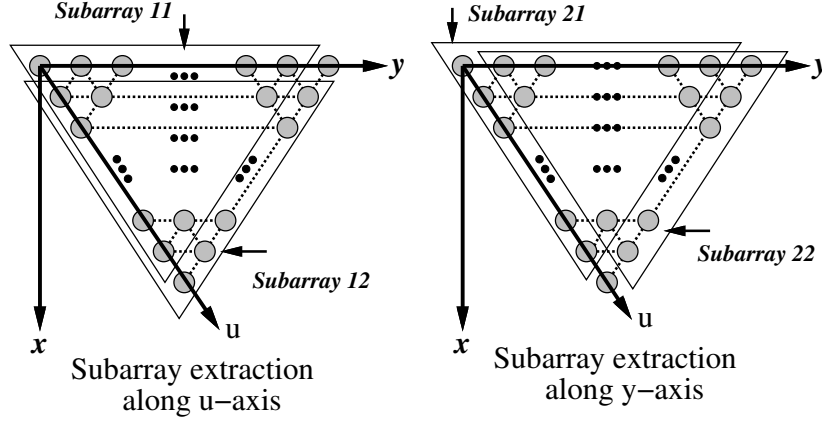


Figure 3: Subarrays in triangular array.

To extract those subarrays, we define first the following $(M_r - 1) \times M_r$ matrices $\mathbf{J}_1^{(M_r)}$ and $\mathbf{J}_2^{(M_r)}$.

$$\mathbf{J}_1^{(M_r)} = \begin{bmatrix} \mathbf{I}_{M_r-1} & \mathbf{O}_{(M_r-1) \times 1} \end{bmatrix}, \quad \mathbf{J}_2^{(M_r)} = \begin{bmatrix} \mathbf{O}_{(M_r-1) \times 1} & \mathbf{I}_{M_r-1} \end{bmatrix} \quad (r = 1, 2) \quad (1)$$

Further, we define “the reduced Kronecker matrix product” denoted by \otimes . This carries out the following matrix operation for \mathcal{A} and \mathcal{B} .

$$\begin{aligned} \mathcal{A} \otimes \mathcal{B} &= \begin{bmatrix} a_{11} & a_{12} & \cdots & a_{1q} \\ a_{21} & a_{22} & \cdots & a_{2q} \\ \vdots & \vdots & & \vdots \\ a_{p1} & a_{p2} & \cdots & a_{pq} \end{bmatrix} \otimes \begin{bmatrix} b_{11} & b_{12} & \cdots & b_{1s} \\ b_{21} & b_{22} & \cdots & b_{2s} \\ \vdots & \vdots & & \vdots \\ b_{r1} & b_{r2} & \cdots & b_{rs} \end{bmatrix} \\ &= \begin{bmatrix} a_{11}b_{11} & \cdots & a_{11}b_{1s} & a_{12}b_{11} & \cdots & a_{12}b_{1s-1} & \cdots & a_{1q}b_{11} \\ \vdots & \vdots & \vdots & \vdots & \vdots & \vdots & \vdots & \vdots \\ a_{11}b_{r1} & \cdots & a_{11}b_{rs} & a_{12}b_{r1} & \cdots & a_{12}b_{rs-1} & \cdots & a_{1q}b_{r1} \\ a_{21}b_{11} & \cdots & a_{21}b_{1s} & a_{22}b_{11} & \cdots & a_{22}b_{1s-1} & \cdots & a_{2q}b_{11} \\ \vdots & \vdots & \vdots & \vdots & \vdots & \vdots & \vdots & \vdots \\ a_{21}b_{r-11} & \cdots & a_{21}b_{r-1s} & a_{22}b_{r-11} & \cdots & a_{22}b_{r-1s-1} & \cdots & a_{2q}b_{r-11} \\ \vdots & \vdots & \vdots & \vdots & \vdots & \vdots & \vdots & \vdots \\ a_{p1}b_{11} & \cdots & a_{p1}b_{1s} & a_{p2}b_{11} & \cdots & a_{p2}b_{1s-1} & \cdots & a_{pq}b_{11} \end{bmatrix} \quad (2) \end{aligned}$$

With this operator \otimes , we make following selection matrices for extracting the four subarrays from the triangular antenna array.

$$\mathbf{J}_{(1)1} \triangleq \mathbf{J}_1^{(M_2)} \otimes \mathbf{J}_1^{(M_1)}, \quad \mathbf{J}_{(1)2} \triangleq \mathbf{J}_1^{(M_2)} \otimes \mathbf{J}_2^{(M_1)} \quad (3)$$

$$\mathbf{J}_{(2)1} \triangleq \mathbf{J}_1^{(M_2)} \otimes \mathbf{J}_1^{(M_1)}, \quad \mathbf{J}_{(2)2} \triangleq \mathbf{J}_2^{(M_2)} \otimes \mathbf{J}_1^{(M_1)} \quad (4)$$

Using the selection matrices of (3) and (4), we can obtain the relationship between the paired subarrays in Fig.3, i.e., the rotational invariance equations as follows:

$$\mathbf{J}_{(r)1} \mathbf{E}_S \Psi_r = \mathbf{J}_{(r)2} \mathbf{E}_S \quad (5)$$

$$\Psi_r \triangleq \mathbf{T}^{-1} \Phi_r \mathbf{T} \quad (r = 1, 2) \quad (6)$$

where \mathbf{E}_S is a signal subspace matrix and can be created via an eigenvalue decomposition (EVD) of the sample correlation matrix of the array[2]. Also, (6) represents the eigenstructure of Ψ_r (\mathbf{T}^{-1} : eigenvector matrix, Φ_r : diagonal eigenvalue matrix). Since Φ_1 and Φ_2 include the 2D-DOA information of the incident waves, we can easily obtain the signal parameters from EVD of Ψ_r ($r = 1, 2$).

2.3 Mean eigenvalue decomposition(MEVD) method

In the multi-dimensional ESPRIT, the estimated signal parameters must be paired signal by signal. In this paper, we employ the MEVD[6] to pair ϕ_i and θ_i for the i th incident wave. From (6), Ψ_1 and Ψ_2 are found to have the following relationship.

$$\Psi_S \triangleq \Psi_1 + \Psi_2 = T^{-1}(\Phi_1 + \Phi_2)T^{-1} \quad (7)$$

Therefore, after calculating the common eigenvector T^{-1} of (7), we can obtain the eigenvalues of Ψ_1 and Ψ_2 as follows:

$$\Phi_1 = T\Psi_1T^{-1}, \quad \Phi_2 = T\Psi_2T^{-1}. \quad (8)$$

This is the MEVD providing the paired 2D-DOA (ϕ_i and θ_i) of all waves.

3 Computer Simulation

We carried out computer simulation to verify the effectiveness of the proposed method. In the simulation, 2D-DOAs are estimated and the estimation accuracy is evaluated using RMSE(Root Mean Square Error) with 100 independent trials. The incident waves are coherent (completely correlated) with each other and the spatial smoothing technique[5] is used as a preprocessing of 2D-ESPRIT. The element spacing is a half wavelength of carrier frequency and the number of element of the triangular array is 15 (one side has 5 elements). The rectangular array with 16 elements is also used for comparison. In the spatial smoothing, the 10-element subarrays(one side has 4 elements) in the triangular array and 9-element subarrays (3×3) in the rectangular array are extracted. SNR of the first wave is 20dB and the number of snapshots for correlation matrix estimation is 30. The scenario of incoming waves (Scenario 1) is presented in Table 1.

The RMSEs of DOA estimates with variation of the azimuth angle of wave 1 are shown in Figs.4 and 5. In the figures, wave 2 keeps 15 degrees apart from wave 1 in azimuth. From Figs.4 and 5, it is found that the triangular array provides almost the same accuracy as the rectangular array, and also that the former reveals the azimuth-independent performance compared to the latter.

Next, the proposed method is compared to the extended ESPRIT[7] that can also make use of the triangular array. The extended ESPRIT is proposed by R.Roy[2] and our method is based on the technique developed by B.Ottersten[3]. The scenario of the incident waves (Scenario 2) is described in Table 2, and the number of elements on a side of the triangular array is increased from 4 to 9. In this simulation, we assume that the two waves are uncorrelated with each other and so the spatial smoothing technique is not employed. Figures 6 and 7 show the RMSEs of DOA estimates versus the number of elements on a side of the triangular array (M_1) in cases of extended ESPRIT and proposed method, respectively. Further, the computation times of both methods are plotted in Fig.8. These figures demonstrate that our method has less computational load than the extended ESPRIT although both have the same estimation accuracy.

4 Conclusion

In this paper, we have proposed 2D-ESPRIT estimator applicable to triangular antenna arrays which cannot be utilized by 2D Unitary ESPRIT. Via computer simulation on 2D-DOA estimation, we have shown that the proposed method reveals azimuth-independent performance compared to the 2D-ESPRIT with the rectangular array. In addition, it is shown that the proposed method has less computational load than the extended ESPRIT which is also applicable to the triangular array.

References

- [1] Y.Ogawa and N.Kikuma: "High-Resolution Techniques in Signal Processing Antennas," IEICE Trans. Commun., Vol.E78-B, No.11, pp.1435–1442, Nov. 1995.
- [2] R.Roy and T.Kailath: "ESPRIT – Estimation of Signal Parameters via Rotational Invariance Techniques," IEEE Trans., Vol.ASSP-37, No.7, pp.984–995, July 1989.

- [3] B.Ottersten, M.Viberg and T.Kailath: “Performance Analysis of the Total Least Squares ESPRIT Algorithm,” IEEE Trans. on Signal Processing, Vol.39, No.5, pp.1122–1135, May 1991.
- [4] Michael D. Zoltowski et al.: “Closed-Form 2-D Angle Estimation with Rectangular Arrays in Element Space or Beamspace via Unitary ESPRIT,” IEEE Trans., Vol.ASSP-44, No.2, pp.316–328, Feb. 1996.
- [5] T.J.Shan, et al.: “On Spatial Smoothing for Direction-of-Arrival Estimation of Coherent Signals,” IEEE Trans., Vol.ASSP-33, No.8, pp.806–811, Aug. 1985.
- [6] N.Kikuma, H.Kikuchi, and N.Inagaki: “Pairing of Estimates Using Mean Eigenvalue Decomposition in Multi-Dimensional Unitary ESPRIT,” IEICE Trans., Vol.J82-B, No.11, pp.2202–2207, Nov. 1999.
- [7] Y.Oh-Hashi and M.Higa: “A Discussion of the Direction Finding System for Moving Radio Sources — Extended ESPRIT Algorithm and Angle Diversity —,” Technical Report of IEICE, AP99-122, pp.119–126, Oct. 1999.

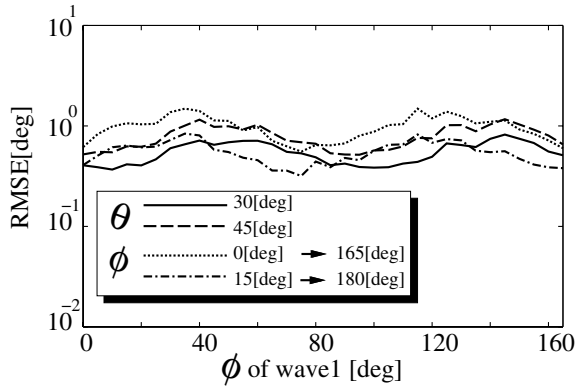


Figure 4: RMSE vs. ϕ of wave 1 (rectangular array)

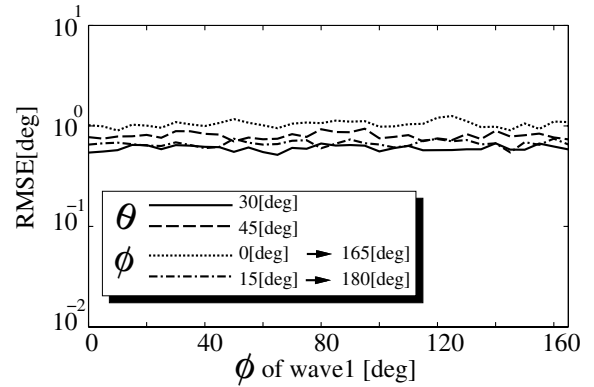


Figure 5: RMSE vs. ϕ of wave 1 (triangular array)

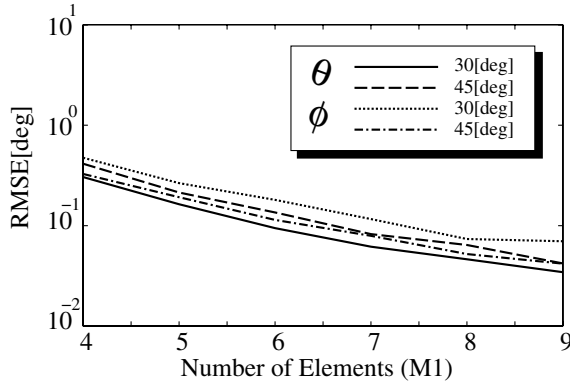


Figure 6: RMSE vs. M_1 (Extended ESPRIT)

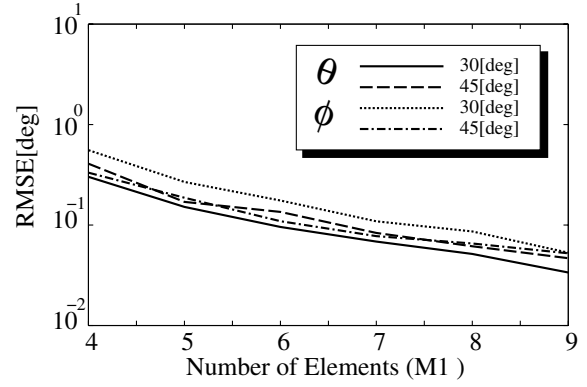


Figure 7: RMSE vs. M_1 (Proposed method)

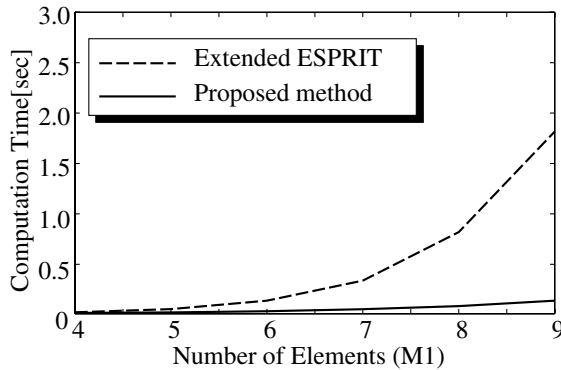


Figure 8: Computation time vs. M_1

Table 1: Radio environment(Scenario 1)

	ϕ [deg]	θ [deg]	power[dB]
wave 1	0 \rightarrow 165	30	0
wave 2	15 \rightarrow 180	45	0

Table 2: Radio environment(Scenario 2)

	ϕ [deg]	θ [deg]	power[dB]
wave 1	30	30	0
wave 2	45	45	0